Supporting Information for "ArchKalMag14k: A Kalman-filter based global geomagnetic model for the Holocene"

M. Schanner[1], M. Korte[1], M. Holschneider[2]

[1]German Research Centre for Geosciences GFZ, Section 2.3, Potsdam, Germany

[2]Applied Mathematics, University of Potsdam, Potsdam, Germany

Contents of this file

Additional Supporting Information (Files uploaded separately)

Introduction

This supplementary material provides validation plots for additional coefficients in Figure S1, a comparison of the model coefficients with the prior in Figure S2 and local field predictions at two additional locations in Figures S3 and S4. Table S1 contains a list of changes made to the GEOMAGIA v.3.4 dataset (Brown et al., 2015). A separately available Movie S1 shows the evolution of the geomagnetic field intensity at the Earth's surface and of the radial component (downwards) at the core mantel boundary, together with respective uncertainties.
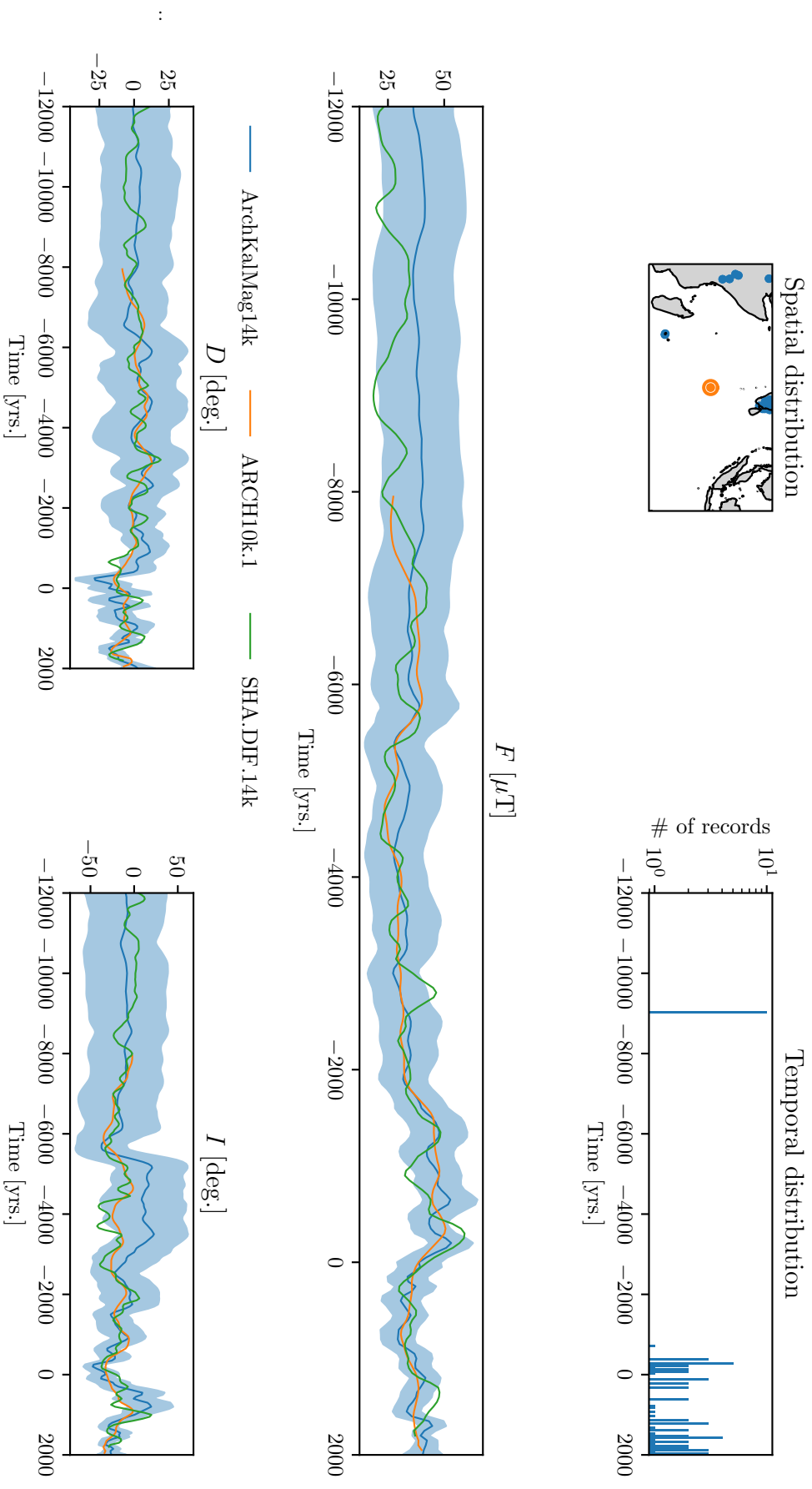
————

September 6, 2021, 5:43am

Figure S3. Local predictions of intensity F, declination D and inclination I for the Indian Ocean. ArchKalMag14k is shown in blue. The shaded area covers 95%. ARCH10k.1 is shown in orange and SHA.DIF.14k in green. In the top row, the spatial and temporal distribution of the surrounding are shown. Data in the orange ellipse (250km radius) are translated to the location of prediction (orange dot) and shown as gray dots. Horizontal and vertical gray bars indicate the one sigma temporal and field component data uncertainties, respectively. The temporal distribution includes all data visible in the left plot.
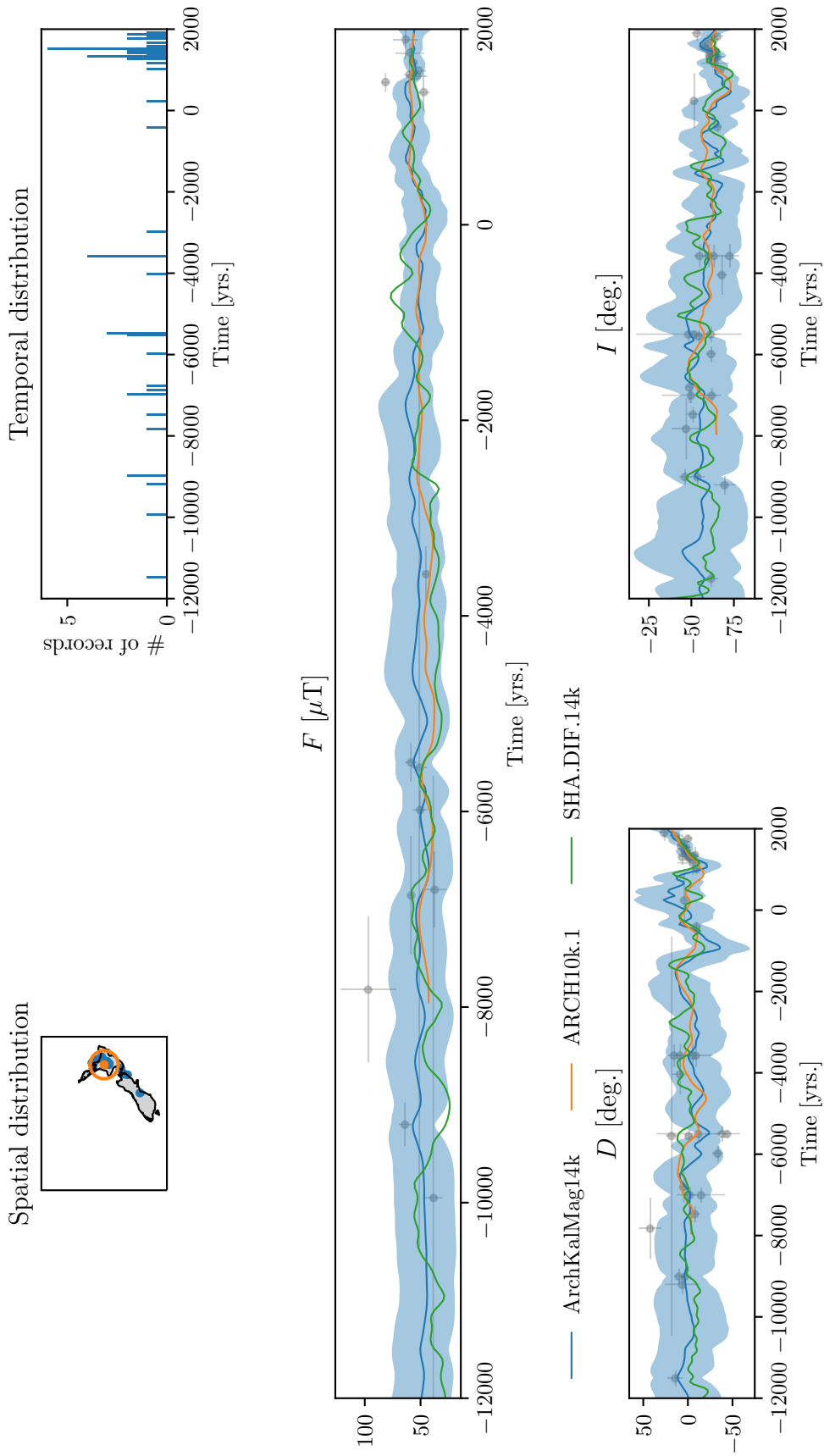
September 6, 2021, 5:43am

Figure S4. Local predictions of intensity F, declination D and inclination I for New Zealand. ArchKalMag14k is shown in blue. The shaded area covers 95%. ARCH10k.1 is shown in orange and SHA.DIF.14k in green. In the top row, the spatial and temporal distribution of the surrounding are shown. Data in the orange ellipse (250km radius) are translated to the location of prediction (orange dot) and shown as gray dots. Horizontal and vertical gray bars indicate the one sigma temporal and field component data uncertainties, respectively. The temporal distribution includes all data visible in the left plot.

Movie S1. Evolution of the geomagnetic field intensity at the Earth's surface (left) and of the radial component (downwards, right) at the core mantel boundary, together with respective uncertainties. The time interval of 50 years corresponds to the full resolution of ArchKalMag14k. Note, that the scales change during the movie. The yellow triangle indicates the location of lowest field intensity. The yellow contour line corresponds to a field value of 32 μT. For reference, both location of lowest intensity and contour are also shown in the CMB plots in blue.

References

Brown, M. C., Donadini, F., Nilsson, A., Panovska, S., Frank, U., Korhonen, K., ... Constable, C. G. (2015). Geomagia50.v3: 2. a new paleomagnetic database for lake and marine sediments. *Earth, Planets and Space*, *67*(1), 70. Retrieved from `https://doi.org/10.1186/s40623-015-0233-z` doi: 10.1186/s40623-015-0233-z
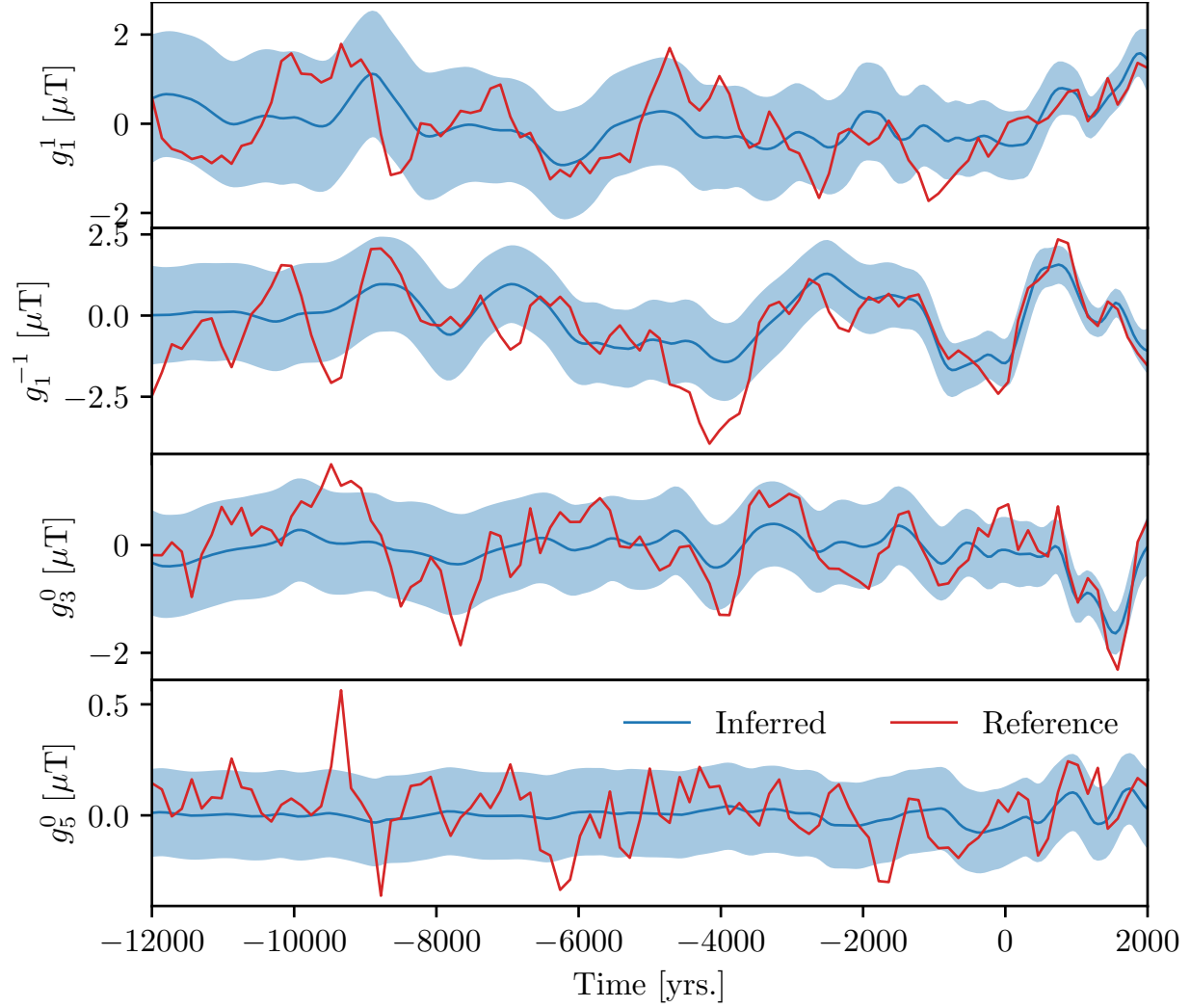
Figure S1. Additional dipole and higher order coefficients of the synthetic model, together with the corresponding inferred ones from the proposed inversion. The inferred (blue) and reference curves (red) agree within the 95%-region shown in light blue.
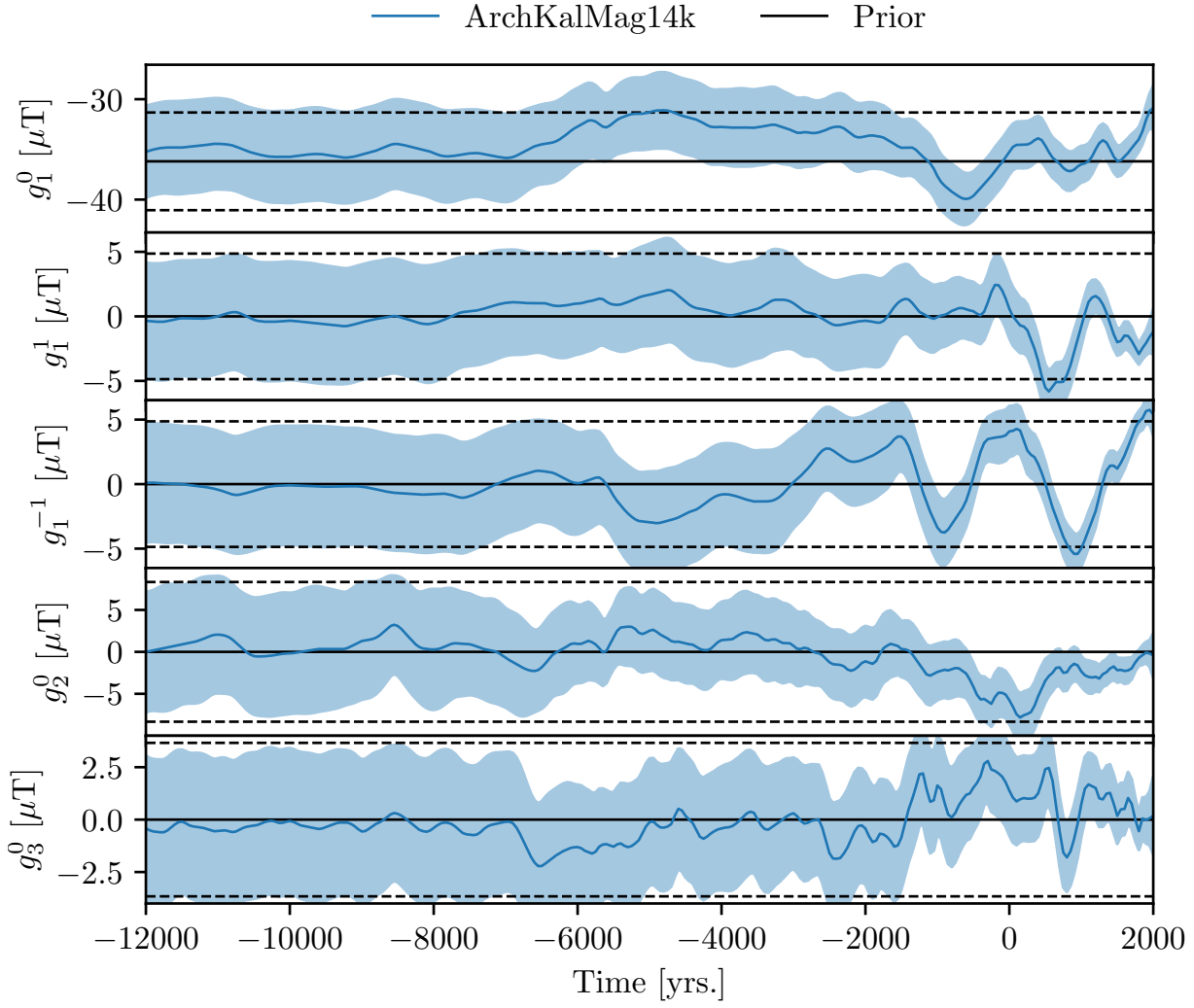
:

Figure S2. ArchKalMag14k model coefficients together with the prior. The shaded area and dashed lines cover 95%.

Table S1. Updates to the GEOMAGIA dataset (Brown et al., 2015) used to assemble the database for ArchKalMag14k. GEOMAGIA provides a unique ID for every record, that we use to identify the records from Mexico that we changed, as they have wrong age and dating uncertainty estimates (Mahgoub, pers. comm.). Records with IDs 11237, 2773, 6891 and 13149 have been removed from the dataset as no updated information is available.

UID	Updated age [yrs.]	Updated standard deviation [yrs.]
13153	-7550	422
2768	-8523	800
2769	-7450	270
11967	-10000	338
6893	-10000	338
11966	-5707	184
2770	1250	5
6892	1250	5
13086	8	62
13118	8	62
11992	1545	94